Investigating Neutron Polarizabilities through Compton Scattering on ³He

Deepshikha Choudhury,[1,2,*] Andreas Nogga,[3] and Daniel R. Phillips[1]

[1]*Department of Physics and Astronomy, Ohio University, Athens, Ohio 45701, USA*
[2]*Department of Physics, George Washington University, Washington D.C. 20052, USA*
[3]*Institut für Kernphysik, Forschungszentrum Jlich, Jlich, Germany*
(Received 5 February 2007; published 7 June 2007)

We examine manifestations of neutron electromagnetic polarizabilities in coherent Compton scattering from the helium-3 nucleus. We calculate γ³He elastic scattering observables using chiral perturbation theory to next-to-leading order $[\mathcal{O}(e^2 Q)]$. We find that the unpolarized differential cross section can be used to measure neutron electric and magnetic polarizabilities, while two double-polarization observables are sensitive to different linear combinations of the four neutron spin polarizabilities.

The theory that describes the internal dynamics of the neutron is quantum chromodynamics (QCD). The neutron has zero charge, but higher electromagnetic moments encode the strong-interaction dynamics which governs its structure. These quantities therefore provide tests of our understanding of QCD. For example, an early success of the $SU(3)$ quark picture was its prediction of magnetic moments, $\vec{\mu}$, for the neutron and other strongly interacting particles (hadrons). Magnetic moments are a first-order response to an applied magnetic field. In this Letter we will be concerned with *electromagnetic polarizabilities*, which quantify the second-order response of a particle to electromagnetic fields. The two most basic polarizabilities

are the electric and magnetic ones, α and β, which measure the ability of an applied electric or magnetic field to produce an induced dipole moment. The Hamiltonian for a neutral particle in applied electric and magnetic fields, $\vec{E}$ and $\vec{B}$, is then

$$H = -\vec{\mu} \cdot \vec{B} - 2\pi[\alpha \vec{E}^2 + \beta \vec{B}^2], \quad (1)$$

where we have worked up to second order in $\vec{E}$ and $\vec{B}$, and have not yet considered terms which involve derivatives of these fields. For a spin-half particle consideration of first-order derivatives allows four new structures which are second order in $\vec{E}$ and $\vec{B}$ [1]. They are

$$-2\pi[(-\gamma_1 - \gamma_3)\vec{\sigma} \cdot \vec{E} \times \dot{\vec{E}} + \gamma_4 \vec{\sigma} \cdot \vec{B} \times \dot{\vec{B}} - (\gamma_2 + \gamma_4)\sigma_i(\nabla_i E_j + \nabla_j E_i)B_j + \gamma_3 \sigma_i(\nabla_i B_j + \nabla_j B_i)E_j]. \quad (2)$$

The coefficients $\gamma_1-\gamma_4$ are the "spin polarizabilities." This Letter will argue that for the neutron, the most basic and stable neutral hadron, α, β, and $\gamma_1-\gamma_4$ can be extracted from Compton scattering on ³He.

Polarizabilities such as those in Eqs. (1) and (2) can be accessed in Compton scattering because the Hamiltonian (1) yields an amplitude for Compton scattering from a neutron target of the form

$$T_{\gamma n} = \sum_{i=1,...,6} A_i^{(n)}(\omega, \theta) t_i. \quad (3)$$

Here t_1-t_6 are invariants constructed out of the photon momenta and polarization vectors ($\hat{\epsilon}$ and $\hat{\epsilon}'$), and, in the case of t_3-t_6, the neutron spin, e.g., $t_1 = \hat{\epsilon}' \cdot \hat{\epsilon}$ and $t_3 = i\vec{\sigma} \cdot (\hat{\epsilon}' \times \hat{\epsilon})$. The A_i's are Compton structure functions. The ω^2 terms of A_1 and A_2 involve α and β [2], while the ω^3 terms of A_3-A_6 depend on $\gamma_1-\gamma_4$ in various combinations.

For the proton, an expression similar to Eq. (3) but supplemented by the Thomson term $-(e^2/M)\hat{\epsilon}' \cdot \hat{\epsilon}$ applies. The larger cross sections that result from the addition of this term lend themselves to low-energy measurements from which $\alpha^{(p)}$ and $\beta^{(p)}$ can be extracted. A considerable number of γp experiments over the past decade had this as

their goal [3]. A combined analysis of their low-energy differential cross section (DCS) data yields [4]

$$\alpha^{(p)} = [12.1 \pm 1.1(\text{stat})]^{+0.5}_{-0.5}(\text{th}) \times 10^{-4}\ \text{fm}^3, \quad (4)$$

$$\beta^{(p)} = [3.4 \pm 1.1(\text{stat})]^{+0.1}_{-0.1}(\text{th}) \times 10^{-4}\ \text{fm}^3. \quad (5)$$

No elastic Compton scattering measurement of the $\gamma_i^{(p)}$'s has yet been performed, but they affect double-polarization observables. Of these, Δ_z and Δ_x are defined by taking the beam helicity to be along $\hat{z}$; then Δ_z (Δ_x) is the difference between the DCS when the target is spin polarized along $+\hat{z}$ ($+\hat{x}$) and along $-\hat{z}$ ($-\hat{x}$). For $\omega < m_\pi$ the $\gamma_i^{(p)}$'s affect Δ_z and Δ_x because of interference between $A_3^{(p)}, \ldots, A_6^{(p)}$ and $A_1^{(p)}$ in the expressions for these observables [5]. An experiment which exploits this interference to probe $\gamma_1^{(p)}-\gamma_4^{(p)}$ has been proposed for the High-Intensity Gamma-ray Source (HI$\vec{\gamma}$S) at TUNL [6].

However, neither polarized nor unpolarized Compton scattering experiments can be directly performed on the neutron, since it is not a stable target. A variety of techniques have been proposed to extract $\alpha^{(n)}$ and $\beta^{(n)}$, including neutron scattering from the Coulomb field of ²⁰⁸Pb and Compton scattering on the deuteron—both elastic and

quasifree. The most accurate numbers come from the last technique and yield (in units of 10^{-4} fm^3) [7]

$$\alpha^{(n)} - \beta^{(n)} = [9.8 \pm 3.6(\text{stat}) \pm 2.2(\text{mod})^{+2.1}_{-1.1}(\text{syst})]. \quad (6)$$

These numbers represent a fascinating interplay of long-distance ($r \sim 1/m_\pi$) and short-distance ($r \sim 1/\Lambda$) dynamics. The dominant piece of $\alpha^{(n)}$ is due to the "cloud" of virtual pions that surrounds the neutron. But there are also significant contributions from short-distance physics—especially in $\beta^{(n)}$. This interplay can be systematically computed in baryon chiral perturbation theory (χPT), a low-energy effective theory that encodes the low-energy symmetries of QCD and the pattern of their breaking (see Ref. [5] for a review). Observables in χPT are computed in an expansion in powers of $Q \equiv p, m_\pi/\Lambda$, where Λ is the excitation energy of the lightest state not explicitly included in the theory. At $\mathcal{O}(e^2Q)$ there are no contributions to the γn amplitude from a short-distance γn operator. The prediction for the γn amplitude comes from nucleon-pole, pion-pole, and one-pion-loop diagrams, with the latter capturing the dominant piece of the "pion cloud." This $\mathcal{O}(e^2Q)$ calculation yields the entire dependence of $A_1^{(n)}$–$A_6^{(n)}$ on photon energy and scattering angle up to corrections of $\mathcal{O}(\frac{\omega}{\Lambda})$. The $\mathcal{O}(\omega^2)$ and $\mathcal{O}(\omega^3)$ nonpole pieces of $A_1^{(n)}$–$A_6^{(n)}$ then give [5,8]

$$\alpha^{(n)} = 10\beta^{(n)} = \frac{5e^2g_A^2}{384\pi^2f_\pi^2 m_\pi} = 12.2 \times 10^{-4} \text{ fm}^3, \quad (7)$$

$$\gamma_1^{(n)} = 2\gamma_2^{(n)} = 4\gamma_3^{(n)} = -4\gamma_4^{(n)} = 4.4 \times 10^{-4} \text{ fm}^4. \quad (8)$$

(The $\gamma_i^{(n)}$'s can also be written in terms of g_A, f_π, and m_π.) The contributions of short-distance physics to Eq. (7) are suppressed by one power of Q, and to Eq. (8) are suppressed by two powers of Q. In addition, χPT predicts that $\alpha^{(p)}$, $\beta^{(p)}$, and the $\gamma_i^{(p)}$'s are the same as the corresponding neutron quantities—at this order. These $\mathcal{O}(e^2Q)$ predictions of χPT agree with the numbers in Eqs. (4) and (6) within the experimental error bars.

We now examine how the predictions of Eqs. (7) and (8) can be tested in elastic γ^3He scattering. The scattering amplitude is written as

$$\mathcal{M} = \langle\Psi_f|\hat{O}|\Psi_i\rangle, \quad (9)$$

with $|\Psi_i\rangle$ and $|\Psi_f\rangle$ being the antisymmetrized ^{3}He wave functions. The results quoted in this Letter have been calculated using a wave function obtained from the Idaho-N^{3}LO chiral potential [9] together with the NNLO chiral $3N$ force [10]. For reviews of χPT applied to nuclear forces, see Ref. [11]. Note, however, that aspects of this power counting are still under discussion [12].

The operator $\hat{O}$ in Eq. (9) is the irreducible amplitude for elastic scattering of real photons from the NNN system, calculated in χPT up to $\mathcal{O}(e^2Q)$. This is next-to-leading order (NLO), a lower order than was used to obtain $|\Psi\rangle$, and so our calculation is chirally consistent only to NLO.

At NLO $\hat{O}$ has a one-body part

$$\hat{O}^{1B} = \hat{O}^{1B}(1) + \hat{O}^{1B}(2) + \hat{O}^{1B}(3), \quad (10)$$

with $\hat{O}^{1B}(a)$ being the γN amplitude where the external photon interacts with nucleon "a." $\hat{O}^{1B}(a)$ (supplemented by what turn out to be very small corrections for the boost from the γN c.m. frame to the γNNN c.m. frame) follows from Eq. (3) and can be found in Refs. [5,13]. Meanwhile the two-body part of $\hat{O}$ is

$$\hat{O}^{2B} = \hat{O}^{2B}(1,2) + \hat{O}^{2B}(2,3) + \hat{O}^{2B}(3,1), \quad (11)$$

and it represents a sum of two-body mechanisms where the external photons interact with the pair "(a, b)." At $\mathcal{O}(e^2Q)$ this operator encodes the physics of two photons coupling to a single pion exchange inside the ^{3}He nucleus. (We do not have to include any irreducible three-body Compton mechanisms in our calculation because they appear at the earliest at $\mathcal{O}(e^2Q^3)$.) We use the expression for $\hat{O}^{2B}$ given in Ref. [13]. This incorporates the few-nucleon physics that corresponds to the pion-cloud dynamics which yields Eqs. (7) and (8). As such it must be included on an equal footing with the polarizability effects that are our focus. The resulting $\hat{O}^{2B}$ gives a significant contribution to the γd cross section, and is an important piece of the χPT calculations that provide a good description of the extant γd DCS data [4,13–15]. We now simplify Eq. (9) to

$$\mathcal{M} = 3\langle\Psi_f|\tfrac{1}{2}[\hat{O}^{1B}(1) + \hat{O}^{1B}(2)] + \hat{O}^{2B}(1,2)|\Psi_i\rangle, \quad (12)$$

using the Faddeev decomposition of $|\Psi\rangle$. The structure of the calculation is then similar for the one- and two-body parts. We calculate $\mathcal{M}$ on a partial-wave Jacobi basis. Convergence of the results with respect to the angular-momentum expansion was confirmed. For details on the calculational procedure, see Ref. [16].

The amplitude (12) is now used to calculate observables. In Fig. 1 we plot our $\mathcal{O}(e^2Q)$ χPT DCS predictions for coherent γ^3He scattering. The two panels are for $\omega = 60$ and 120 MeV. Both show three different DCS calculations—$\mathcal{O}(e^2)$, impulse approximation (IA), and $\mathcal{O}(e^2Q)$. The $\mathcal{O}(e^2)$ calculation includes only the proton Thomson term, since that is the γN amplitude in χPT at that order.
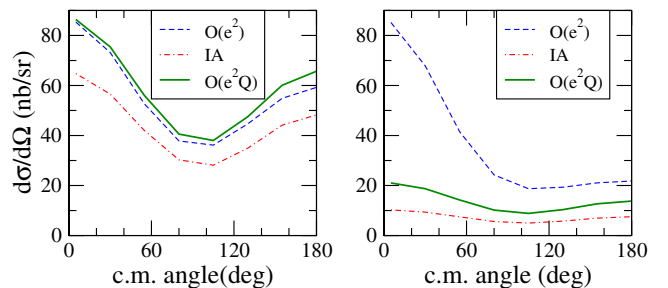

FIG. 1 (color online). Comparison of different c.m.-frame DCS calculations at 60 MeV (left panel) and 120 MeV (right panel).
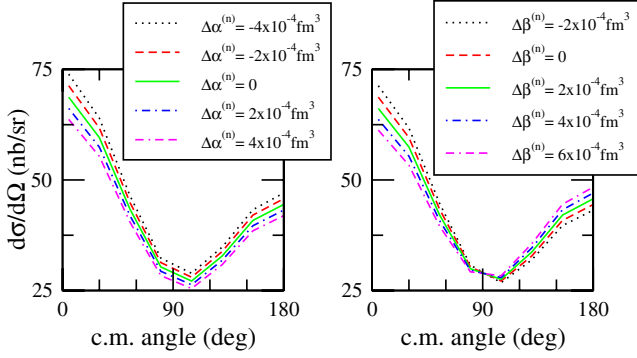
FIG. 2 (color online).　The c.m.-frame $\mathcal{O}(e^2 Q)$ DCS at 80 MeV with varying $\Delta \alpha^{(n)}$ (left panel) and $\Delta \beta^{(n)}$ (right panel).

The IA calculation is done up to $\mathcal{O}(e^2 Q)$ but does not have any two-body contribution. As expected, we see that there is a sizable difference between the IA and the $\mathcal{O}(e^2 Q)$ DCS: the two-body currents are important and cannot be neglected. Also, we see that the difference between $\mathcal{O}(e^2)$ and $\mathcal{O}(e^2 Q)$ is very small at 60 MeV—showing that χPT may converge well there—and gradually increases with energy. This is partly because the fractional effect of $\alpha^{(n)}$ and $\beta^{(n)}$ increases with ω.

To quantify this, in Fig. 2 we plot the $\mathcal{O}(e^2 Q)$ DCS at 80 MeV obtained when we add shifts, $\Delta \alpha^{(n)}$ and $\Delta \beta^{(n)}$, to the $\mathcal{O}(e^2 Q)$ values of the neutron electric and magnetic polarizabilities (7). We take $\Delta \alpha^{(n)}$ in the range $(-4, \ldots, 4) \times 10^{-4}$ fm^3 and $\Delta \beta^{(n)}$ between $(-2, \ldots, 6) \times 10^{-4}$ fm^3. This allows us to assess the impact that one set of higher-order mechanisms has on our $\mathcal{O}(e^2 Q)$ predictions. Two features of Fig. 2 are particularly notable. First, sensitivity to $\beta^{(n)}$ vanishes at $\theta = 90°$ because $\alpha^{(n)}$ and $\beta^{(n)}$ enter $A_1^{(n)}$ in the combination $\alpha^{(n)} + \beta^{(n)} \cos\theta$. Thus, $\alpha^{(n)}$ and $\beta^{(n)}$ can be extracted independently from the same experiment. Second, the absolute size of the shift in the DCS due to $\Delta \alpha^{(n)}$ and $\Delta \beta^{(n)}$ is roughly the same for all energies. This suggests that measurements could be done at $\omega \approx 80$ MeV, where the count rate is higher, and the contribution of higher-order terms in the chiral expansion should be smaller.

We have estimated the uncertainty due to short-distance physics in the three-nucleon system by using a variety of ^{3}He wave functions generated using various NN interac-

tions with and without a corresponding 3N force. This produced changes of $\lesssim 15\%$ in the DCS at 120 MeV.

Before examining double-polarization observables in γ^3He scattering we try to develop some intuition for the γ^3He amplitude. Since ^{3}He is a spin-$\frac{1}{2}$ target the matrix element (12) can be decomposed in the same fashion as was the neutron's Compton matrix element in Eq. (3).

$$ T_{\gamma^3 \text{He}} = \sum_{i=1,\ldots,6} A_i^{3\text{He}}(\omega, \theta) t_i; \qquad A_i^{3\text{He}} = A_i^{1B} + A_i^{2B}, \quad (13) $$

where A_i^{1B} (A_i^{2B}) comes from considering the matrix element of the one-body (two-body) operators in Eq. (12), and the structures t_3–t_6 now involve the nuclear—not the neutron—spin. However, in ^{3}He the two proton spins are—to a good approximation—antialigned, so the nuclear spin is largely carried by the unpaired neutron [17]. We find that the $\mathcal{O}(e^2 Q)$ two-body currents A_1^{2B} and A_2^{2B} are numerically sizable, but A_3^{2B}–A_6^{2B} are negligible. Hence, to the extent that polarized ^{3}He is an effective neutron, we expect $A_i^{3\text{He}} = A_i^{(n)}$ for $i = 3$–6. Using Eq. (13) to translate this into predictions for Δ_z and Δ_x shows that the effects of $\gamma_1^{(n)}$–$\gamma_4^{(n)}$ will be enhanced in these observables by interference with $A_1^{3\text{He}}$. But $A_1^{3\text{He}}$ is—at least at $\omega \approx 80$ MeV—dominated by the contribution of the two protons, and so we anticipate a more marked signal from the neutron spin polarizabilities than is predicted for the corresponding γd observables [18].

We emphasize that these arguments are meant only as a guide to the physics of our exact $\mathcal{O}(e^2 Q)$ calculation. Our ^{3}He wave function is obtained by solving the Faddeev equations with NN and 3N potentials derived from χPT. All of the effects due to neutron depolarization and the spin-dependent pieces of $\hat{O}^{2B}$ are included in our calculation of the amplitude (9). This yields the results for Δ_z and Δ_x shown in Figs. 3 and 4. There we have proceeded analogously to our computations of the γ^3He DCS, this time varying the neutron spin polarizabilities and seeing the effect on Δ_z and Δ_x. Figure 3 indicates that Δ_z is quite sensitive to $\gamma_1^{(n)}$, $\gamma_2^{(n)}$, and $\gamma_4^{(n)}$. With the expected photon flux at an upgraded HI$\vec{\gamma}$S such effects can be measured [19]. If this can be done as a function of θ we can extract the combination $\gamma_1^{(n)} - (\gamma_2^{(n)} + 2\gamma_4^{(n)}) \cos\theta$. Turning to Δ_x, Fig. 4 shows that varying $\gamma_1^{(n)}$ or $\gamma_4^{(n)}$ produces appreciable
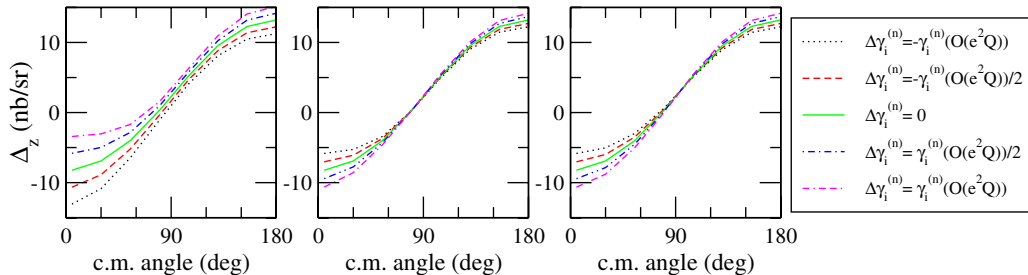

FIG. 3 (color online).　Δ_z at $\omega = 120$ MeV with (left to right) $\gamma_1^{(n)}$, $\gamma_2^{(n)}$, and $\gamma_4^{(n)}$ varied one at a time. For $\mathcal{O}(e^2 Q)$ $\gamma_i^{(n)}$'s, see Eq. (8).
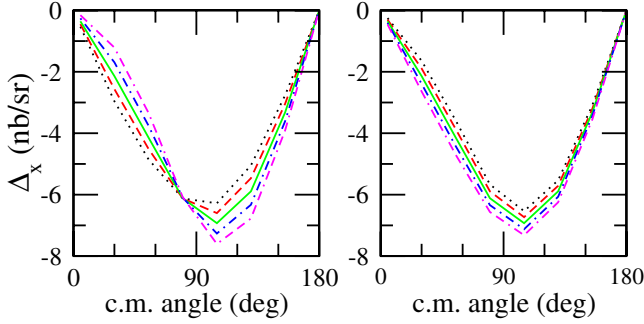
P H Y S I C A L R E V I E W L E T T E R S

FIG. 4 (color online). Δ_x (c.m. frame) at $\omega = 120$ MeV when $\gamma_1^{(n)}$ (left) and $\gamma_4^{(n)}$ (right) are varied one at a time. Legend as in Fig. 3.

effects in Δ_x—but in a different combination to the sensitivity in Δ_z. Use of different ^{3}He wave functions alters these predictions for Δ_x and Δ_z by $\lesssim 7.5\%$. For a more detailed discussion see [16]. Thus, Δ_z and Δ_x are sensitive to two different linear combinations of $\gamma_1^{(n)}$, $\gamma_2^{(n)}$, and $\gamma_4^{(n)}$ and their measurement should provide an unambiguous extraction of $\gamma_1^{(n)}$, as well as constraints on $\gamma_2^{(n)}$ and $\gamma_4^{(n)}$.

These γ^3He scattering calculations are the first calculations for this reaction, and there is significant scope for improvement. Computing of the NNLO [$\mathcal{O}(e^2Q^2)$] pieces of the γNNN operator $\hat{O}$ would allow a more detailed assessment of the pattern of convergence. When this is done we anticipate three kinematic domains where convergence may be slow. First, since we use the heavy-baryon formulation of χPT, the pion-production threshold is at $\omega = m_\pi$, rather than in the correct position for γ^3He scattering which is $\sim$4 MeV lower. An estimate of the impact of this discrepancy on observables suggests a $\sim$5% difference in the DCS, and $\lesssim 3\%$ in Δ_z and Δ_x, at 100 MeV. Second, the power counting we used is not valid at energies $\lesssim m_\pi^2/M$. For instance, it does not reproduce the correct $\omega = 0$ (Thomson) limit for the nuclear target, since the terms in $\hat{O}$ that restore that limit are higher-order effects when $\omega \sim m_\pi$. (A recent computation for γd scattering verifies that they are indeed small for $\omega \gtrsim 80$ MeV [15].) We therefore expect that assessment of these two classes of corrections, while an important check on our results, will not significantly alter them. We believe that the most important correction will come from the inclusion of $\Delta(1232)$ degree of freedom. γd scattering calculations which included such effects found a sizable impact on the DCS at backward angles for $\omega \approx 100$ MeV [14].

Our results for γ^3He scattering are obtained from χPT NN and NNN interactions and γN and γNN operators, and are accurate to NLO in the chiral expansion. These first results on this reaction suggest that $\alpha^{(n)}$ and $\beta^{(n)}$ can be extracted from the γ^3He DCS and compared to results from γd experiments at MAXLab [20]. Meanwhile, two different linear combinations of $\gamma_1^{(n)}$, $\gamma_2^{(n)}$, and $\gamma_4^{(n)}$ can be constrained by measurements of double-polarization ob-

servables at facilities such as HI$\vec{\gamma}$S. This would provide new information on neutron polarizabilities.

We thank H. Gao, A. Nathan, and L. Platter for useful conversations. This work was carried out under Grant No. DE-FG02-93ER40756 of the U.S. DOE and NSF Grant No. PHY-0645498 (D. C.). The wave functions have been computed at the NIC, Jülich.

*Electronic address: choudhur@phy.ohiou.edu

[1] S. Ragusa, Phys. Rev. D **47**, 3757 (1993); B. R. Holstein, D. Drechsel, B. Pasquini, and M. Vanderhaeghen, Phys. Rev. C **61**, 034316 (2000).
[2] These ''Compton'' polarizabilities equal the ''static'' ones [Eq. (1)] only in the nonrelativistic limit, but the ~5% difference is understood and calculable.
[3] For a recent review, see M. Schumacher, Prog. Part. Nucl. Phys. **55**, 567 (2005).
[4] S. R. Beane *et al.*, Phys. Lett. B **567**, 200 (2003).
[5] V. Bernard, N. Kaiser, and Ulf-G. Meißner, Int. J. Mod. Phys. E **4**, 193 (1995).
[6] R. Miskimen, in Proceedings of the 5th International Workshop on Chiral Dynamics, Theory and Experiment, Durham, NC, 2006 (World Scientific, Singapore, to be published).
[7] K. Kossert *et al.*, Eur. Phys. J. A **16**, 259 (2003).
[8] V. Bernard, N. Kaiser, and Ulf-G. Meißner, Phys. Rev. Lett. **67**, 1515 (1991).
[9] D. R. Entem and R. Machleidt, Phys. Rev. C **68**, 041001 (2003).
[10] U. van Kolck, Phys. Rev. C **49**, 2932 (1994); A. Nogga, P. Navratil, B. R. Barrett, and J. P. Vary, Phys. Rev. C **73**, 064002 (2006).
[11] P. F. Bedaque and U. van Kolck, Annu. Rev. Nucl. Part. Sci. **52**, 339 (2002); E. Epelbaum, Prog. Part. Nucl. Phys. **57**, 654 (2006).
[12] S. R. Beane, P. F. Bedaque, M. J. Savage, and U. van Kolck, Nucl. Phys. **A700**, 377 (2002); A. Nogga, R. G. E. Timmermans, and U. van Kolck, Phys. Rev. C **72**, 054006 (2005); E. Epelbaum and Ulf-G. Meißner, arXiv:nucl-th/0609037.
[13] S. R. Beane, M. Malheiro, D. R. Phillips, and U. van Kolck, Nucl. Phys. **A656**, 367 (1999).
[14] R. P. Hildebrandt, H. W. Grießhammer, T. R. Hemmert, and D. R. Phillips, Nucl. Phys. **A748**, 573 (2005).
[15] R. P. Hildebrandt, H. W. Grießhammer, and T. R. Hemmert, arXiv:nucl-th/0512063.
[16] D. Choudhury, D. R. Phillips, and A. Nogga (to be published); D. Choudhury, Ph.D. thesis, Ohio University, 2006.
[17] B. Blankleider and R. M. Woloshyn, Phys. Rev. C **29**, 538 (1984); J. L. Friar *et al.*, Phys. Rev. C **42**, 2310 (1990).
[18] D. Choudhury and D. R. Phillips, Phys. Rev. C **71**, 044002 (2005).
[19] H. Gao, in Proceedings of the 5th International Workshop on Chiral Dynamics, Theory and Experiment, Durham, NC, 2006 (Ref. [6]).
[20] K. Fissum, in Proceedings of the 5th International Workshop on Chiral Dynamics, Theory and Experiment, Durham, NC, 2006 (Ref. [6]).